Macroscopic Alignment of Concentrated Block Copolymer Solutions in Electric Fields

Alexander Böker[a,b], Hubert Elbs[a], Helmut Hänsel[a], Armin Knoll[a], Sabine Ludwigs[a], Heiko Zettl[a], Volker Urban[d], Volker Abetz[b], Axel H. E. Müller[b,c], and Georg Krausch[a,c]*

[a] Lehrstuhl für Physikalische Chemie II,
[b] Lehrstuhl für Makromolekulare Chemie II and
[c] Bayreuther Zentrum für Kolloide und Grenzflächen,
Universität Bayreuth, D-95440 Bayreuth, Germany
[d] European Synchrotron Radiation Facility (ESRF), F-38043 Grenoble, France

Introduction

In addition to mechanical fields, the potential of *electric fields* for microdomain alignment has attracted increasing interest in the recent past[1]. It has been shown that both lamellar and cylindrical microdomain structures in polystyrene-*b*-poly(methyl methacrylate) (PS-*b*-PMMA) thin films could be oriented by virtue of a d.c. electric field [2 - 8]. These *melt* based electric field procedures suffer from limitations associated with the high melt viscosities typical of high molecular weight copolymers or copolymers of more complex architectures. In order to overcome these limitations, one can try to align concentrated block copolmyer solutions, where a non-selective solvent is used to induce sufficient mobility. Following earlier investigations by Le Meur *et al.*[9] we recently investigated the microdomain alignment of an ABC triblock copolymer during solvent casting in the presence of an external electric d.c. field[10]. After drying, bulk samples of the material exhibited lamellar microdomains highly oriented parallel to the electric field vector, as shown by small angle X-ray scattering (SAXS) and transmission electron microscopy (TEM). In the present paper, we describe recent real-time synchrotron radiation small angle X-ray scattering (Synchrotron-SAXS) investigations aiming to follow the kinetics of electric field induced microdomain reorientation in concentrated block copolymer solutions and to elucidate the underlying microscopic mechanisms.

Experimental

Materials and Experimental Setup. A polystyrene-*b*-polyisoprene block copolymer (SI) was synthesized by sequential living anionic polymerization [11]. The polymer consists of 52 wt% polystyrene and 48 wt% polyisoprene (92% 1,4-cis and 4% 1,2 and 3,4 microstructure) with a total number average molecular weight M_n = 80 kg/mol and a polydispersity M_w/M_n = 1.02.

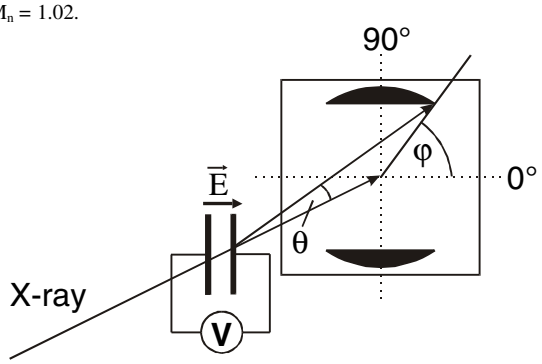

Figure 1. Experimental Setup for in-situ SAXS.

Toluene solutions of the block copolymer with concentrations ranging from 30 - 80 wt% were prepared. The alignment experiments were performed in a home built capacitor with gold electrodes (sample depth = 5 mm, electrode distance d = 2 mm) at temperatures ranging from room temperature to 80°C. A d.c. voltage between 0.5 and 6 kV was applied across the capacitor resulting in a homogeneous electric field pointing perpendicular to the X-ray beam direction (Figure 1). Both the voltage at the electrodes and the current through the sample were monitored during the course of the experiment. No leakage currents were detected after the electric field was applied. The sample temperature was adjusted to within ±1 °C using Peltier elements.

Synchrotron-SAXS measurements were performed at the ID2A beamline at the European Synchrotron Radiation Facility (ESRF, Grenoble, France). The diameter of the X-ray beam was 200 µm. The photon energy was set to 12.5 keV, corresponding to an X-ray wavelength of 0.1 nm. SAXS spectra were recorded with a two-dimensional camera located at a distance of some 10 m to the sample within an evacuated flight tube. The detector can monitor up to 10 frames (1024x1024 pixels) per second and a sequence of up to 125 frames can be acquired with this time resolution.

Results and Discussion

Orientation Mechanisms. Interestingly, at zero electric field the microdomain structure appears to be highly oriented parallel to the electrodes. This can be seen in the azimuthal angular dependence of the scattering intensity of the (100) peak displayed in Figure 2A which shows two distinct peaks around $\varphi = 0°$ and $\varphi = 180°$. This behavior is found immediately after filling the sample chamber and is retained after heating the sample above the order-disorder temperature and subsequent cooling. We therefore anticipate that preferential attraction of the PS block to the gold surfaces is responsible for this alignment[12].

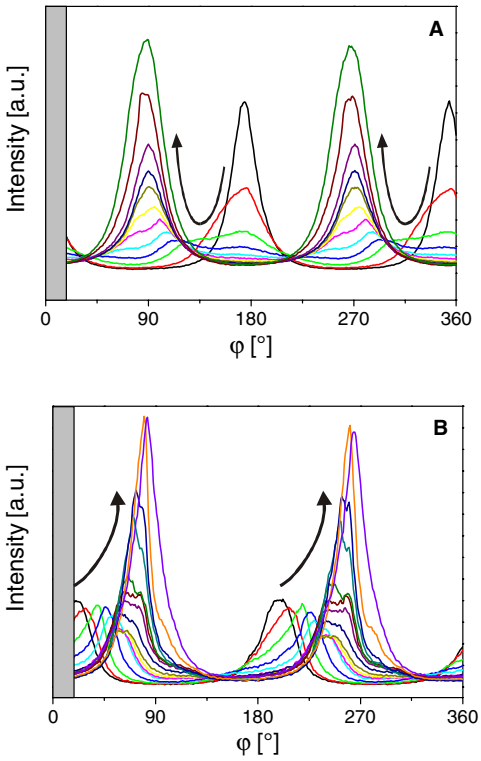

Figure 2. Evolution of the azimuthal angular dependence of the scattering intensity with time for different concentrations at 2kV/2mm. (A) 35 wt.-%, (B) 50 wt.-%. The arrows indicate the course of pattern evolution with time.

If an electric field is applied across the two gold electrodes, the scattering pattern changes significantly. As can be seen from the azimuthal angular dependence of the scattering intensity at different times after switching on the d.c. voltage, the anisotropic pattern first turns into a nearly isotropic ring of weak intensity (Figure 2A, blue curve) before two distinct peaks are formed at around $\varphi = 90°$ and $\varphi = 270°$ at later times. Clearly an almost complete destruction of the initial peaks is seen at early times followed by the built-up of new peaks at around $\varphi = 90°$ and $\varphi = 270°$, respectively.

Before we turn to a quantitative discussion of the kinetic data we note that a *qualitatively* different reorientation behavior is observed if the polymer concentration is significantly increased. This is shown in Figure 2B for a polymer solution with ϕ_{pol} = 50 wt%. In contrast to the situation described above, the initial scattering peaks are not destroyed as the electric field is applied, however, they merely rotate from their original positions at $\varphi = 0°$ and $\varphi = 180°$ towards their final positions at $\varphi = 90°$ and $\varphi = 270°$, respectively. The peak intensities decrease slightly during the rotation process and eventually increase again after the final orientation has been reached. For

intermediate concentrations (not shown here), a superposition of both behaviors is observed.

These findings point to two different underlying mechanisms responsible for microdomain reorientation in the presence of the electric field. Close to the ODT, i.e. at low concentrations and high temperatures, microdomains aligned parallel to the electric field grow at the expense of those aligned parallel to the electrodes. Intermediate orientations, however, are not observed. This behavior matches the notion of the *migration of grain boundaries*, which has previously been described for microdomain alignment under shear[13] and which was assumed to play a role in electric field experiments as well[2,3]. In this case, one lamella grows at the expense of another with a significantly different orientation by motion of a tilt boundary (wall defect) between them, leading to a direct transfer of scattering intensity between widely separated azimuthal angles φ.

Further away from the ODT, i.e. for high concentrations and low temperatures, the scattering pattern seems to be preserved and merely shifts into the new orientation. This observation points to the *rotation of entire grains* as an alternative orientation process. In contrast to the migration of grain boundaries, microdomain orientations intermediate between the original and the final orientations are observed. At the same time no increase in isotropic scattering is observed. Nevertheless, the peak intensity decreases temporarily and is recovered only after the final orientation is reached. This decrease indicates that the grains do not necessarily rotate around the electric field direction, but rather around arbitrary axes.

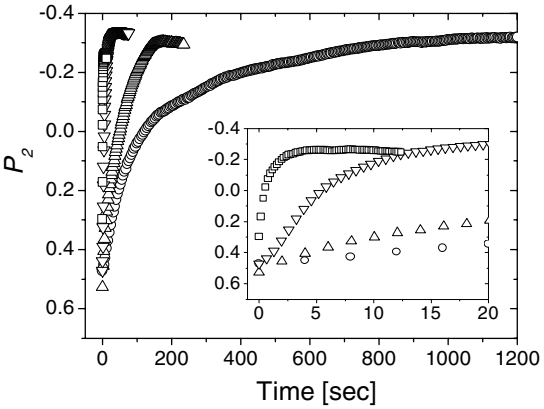

Figure 3. Evolution of orientational order parameter P_2 with time for different concentrations at 2kV/2mm (□ = 34.5 wt.-%, ▽ = 37.5 wt.-%, △ = 42.5 wt.-%, ○ = 50 wt.-%).

Orientation Kinetics. In order to quantify the degree of microdomain alignment, we calculate the order parameter P_2 by integrating the scattering intensity I_q from φ = 0° to 360°:

$$P_2 = \frac{3\langle \cos^2 \varphi \rangle - 1}{2}$$

with

$$\langle \cos^2 \varphi \rangle = \frac{\int_0^{2\pi} d\varphi \left(I_q(\varphi) \cdot \cos^2(\varphi) \cdot |\sin(\varphi)| \right)}{\int_0^{2\pi} d\varphi \left(I_q(\varphi) \cdot |\sin(\varphi)| \right)}$$

For lamellar alignment parallel to the electrodes, P_2 ranges from 0 to 1 with $P_2 = 1$ corresponding to perfect parallel alignment of the lamellae. For an alignment of the lamellae along the field direction, P_2 ranges from 0 to -0.5. Here, $P_2 = -0.5$ corresponds to the case where all lamellae are aligned parallel to the field, however, with the lamella normals being isotropically oriented in the plane of the electrodes. The time development of P_2 can be represented by a single exponential $P_2(t) = P_{2,\infty} + (P_{2,0} - P_{2,\infty}) \exp(-t/\tau)$, where $P_{2,0}$ and $P_{2,\infty}$ are the limiting values of the order parameter in the absence and the presence of the electric field, respectively, and τ is a time constant describing the kinetic behavior.

With increasing polymer concentration the time constant τ increases as can be seen in Figure 3. Simultaneously we also observe an increase in viscosity of the respective systems. The viscosity only influences the kinetics but not the final degree of order ($P_{2,\infty}$), which is consistent with previous dielectric relaxation spectroscopy measurements on the realignment of a side-chain liquid crystalline polymer in its liquid-crystalline state induced by a d.c. electric field[14].

Conclusions

We have shown that real-time synchrotron SAXS measurements provide insight into the microscopic processes relevant for microdomain alignment in concentrated block copolymer solutions. Close to the ODT, *migration of grain boundaries* seems to be the dominant mechanism, while *rotation of grains* dominates further away from the ODT, i.e. under strongly segregating conditions. The rather fast reorientation kinetics could be resolved and quantified.

Acknowledgements. The authors would like to acknowledge financial support by the *Verband der Chemischen Industrie (VCI)* and the German *Bundesministerium für Bildung und Forschung (BMBF)*. We are grateful to the *ESRF* for financial support and provision of synchrotron beam time. This work was carried out in the framework of the *Sonderforschungsbereich 481* funded by the *German Science Foundation (DFG)*.

References

(1) Thurn-Albrecht, T.; Schotter, J.; Kastle, G.A.; Emley, N.; Shibauchi, T.; Krusin-Elbaum, L.; Guarini, K.; Black, C.T.; Tuominen, M.T.; Russell, T.P. *Science* **2000**, *290*, 2126.
(2) Amundson, K.; Helfand, E.; Davis, D.D.; Quan, X.; Patel, S.S.; Smith, S.D. *Macromolecules* **1991**, *24*, 6546.
(3) Amundson, K.; Helfand, E.; Quan, X.; Smith, S.D. *Macromolecules* **1993**, *26*, 2698.
(4) Morkved, T.L.; Lu, M.; Urbas, A.M.; Ehrichs, E.E.; Jaeger, H.M.; Mansky, P.; Russell, T.P. *Science* **1996**, *273*, 931.
(5) Morkved, T.L.; Lopez, V.A.; Hahm, J.; Sibener, S.J.; Jaeger, H.M. *Polymer* **1998**, 39, 3871.
(6) Mansky, P.; DeRouchey, J.; Russell, T.P.; Mays, J.; Pitsikalis, M.; Morkved, T.L.; Jaeger, H.M. *Macromolecules* **1998**, *31*, 4399.
(7) Thurn-Albrecht, T.; DeRouchey, J.; Russell, T.P.; Jaeger, H.M. *Macromolecules* **2000**, *33*, 3250.
(8) Amundson, K.; Helfand, E.; Quan, X.; Hudson, S.D.; Smith, S.D. *Macromolecules* **1994**, *27*, 6559.
(9) Le Meur, J.; Terrisse, J.; Schwab, C.; Goldzene, P. *J. Phys., Colloq.* **1971**, *32*, C5a-301.
(10) Böker, A.; Knoll, A.; Elbs, H.; Abetz, V.; Müller, A.H.E.; Krausch, G. *Macromolecules* **2002**, *35*, 1319.
(11) Schmalz, H.; Böker, A.; Lange, R.; Krausch, G.; Abetz, V. *Macromolecules* **2001**, *34*, 8720.
(12) Anastasiadis, S.H.; Russell, T.P.; Satija, S.K. *Phys. Rev. Lett.* **1989**, *62*, 1852.
(13) Polis, D.L.; Smith, S.D.; Terrill, N.J.; Ryan, A.J.; Morse, D.C.; Winey, K.I. *Macromolecules* **1999**, *32*, 4668.
(14) Kozak, A.; Simon, G.P.; Moscicki, J.K.; Williams, G. *Mol. Cryst. Liq. Cryst.* **1990**, *193*, 155.